

## Effect of Reactive Magnesium Oxide on Properties of Alkali Activated Slag Geopolymer Cement Pastes

H.A. Abdel-Gawwad\*

Housing and Building National Research Center, Cairo, Egypt

\*E-mail: [hamdyabdelgawwad@yahoo.com](mailto:hamdyabdelgawwad@yahoo.com)

### ABSTRACT

The effect of different proportions and different reactivities of MgO on the drying shrinkage and compressive strength of alkali activated slag pastes (AAS) has been investigated. The slag was activated by 6 wt. % sodium hydroxide and liquid sodium silicate at ratio of 3:3 wt %. The different reactivities of MgOs were produced from the calcination of hydromagnesite at different temperatures (550, 1000, 1250 °C). The results showed that the reactivity of magnesium oxide decreases with increasing the calcination temperature. Also, the drying shrinkage of AAS was reduced by the replacement of slag with MgOs. The highly reactive MgO accelerated the hydration of AAS at early ages. The replacement of slag with 5% MgO<sub>550</sub> increased one day compressive strength by ~26% while MgO<sub>1250</sub> had little effect. A significant increase in strength was observed after 7 days in case of replacement of slag with 5 % MgO<sub>1250</sub>. The MgO reacts with slag to form hydrotalcite like- phases (Ht) as detected by XRD, FTIR spectroscopy, TGA/DTG analysis and SEM.

**Keywords:** reactive magnesium oxide, calcination temperature, drying shrinkage, hydrotalcite like-phases, magnesium silicate hydrate.

### 1. INTRODUCTION

Alkali-activated slag (AAS) binders have taken a great interest due to its manufacturing process which has important benefits from the point of view of the lower energy requirements and lower emission of greenhouses gases with respect to the manufacturing of Portland cement. Several studies (**Fernández et al. 1999; Cahit et al. 2010; El-Didamony et al. 2012**) indicate that AAS cements and concretes present high mechanical strength and good performance in chemical attack, frost-thaw cycles and high temperatures. The main application of these binders is in pre-casting and repairing. However, previous researches (**Cincotto et al. 2003; Collins and Sanjayan 1996**) have shown that alkali activated slag mortars and concretes are subject to substantial autogenous and drying shrinkage. This is one of the main drawbacks to the definitive use of AAS as an alternative to traditional Portland cement binders.

There are a number of factors that determine the drying shrinkage of AAS including the type and content of the alkali activators (**Shi 1996; Shi and Day 1996**), properties of the aggregate and the slag (**Cincotto et al. 2003**), as well as curing environment (**Hikkinen 1993; Li and Sun 2000**). In general, water-glass activated slag has more shrinkage than sodium hydroxide activated slag and the drying shrinkage of AAS

increases with increasing dosage of activators as well as slag fineness (**Krizan and Zivanovic 2002; Melo et al. 2008**). In addition, the shrinkage of AAS is very sensitive to the curing environment. It is reported that although at 70% RH the drying shrinkage of AAS concrete is similar to that of PC concrete (**Kutti et al. 1992**), and it is significantly higher at 33% and 50% RH (**Kutti et al. 1992; Douglas et al. 1992**).

Some authors (**Wittmann 1982; Young 1988**) suggested that the characteristics of hydrated calcium silicate gel and pore size distribution, have a direct effect on the drying shrinkage. According to Kutti (**1992**) two main hydration products are formed as a result of alkali activation of slag, a C–S–H gel similar to the gel formed in Portland cement pastes, although with a lower Ca/Si ratio, and a Si-rich gel with properties similar to silica gel. This latter product contains higher free water content that is eliminated during the drying process, causing substantial shrinkage and therefore microcracking.

In order to reduce the drying shrinkage of AAS concrete, Bakharev et al. (**2000**) investigated the effect of different admixtures on water glass-activated slag concrete. Lower drying shrinkage (at 50% RH) was observed for the AAS compared to PC concrete prepared with 6% gypsum and concluded that gypsum reduces both autogenous and drying shrinkage due to the formation of expansive phases such as ettringite (AFt). Specimens with superplasticizer showed the highest drying shrinkage, followed by without admixtures and then with water-reducing admixtures, whilst the specimens containing air-entraining agent exhibited the lowest shrinkage. On the other hand, the compressive strength results showed that superplasticiser admixture resulted in a 25% loss of 28 day strength and water reducing (based on lignosulphonates) reduced the early strength up to 14 days, while the air-entraining agent had no negative effect (**Bakharev et al. 2000**). They concluded that it was not desirable to use superplasticiser in AAS concretes, which is consistent with other findings that some of the conventional admixtures used for PC have detrimental effects in AAS concrete (**Rashad 2013**).

. Palacios and Puertas (**2007**) investigated the effect of polypropylenglycol-based shrinkage-reducing admixture (SRA) on the drying shrinkage of water glass-activated slag mortars. They reported that 1% and 2% SRA reduced drying shrinkage by 7% and 50% respectively at 50% RH, while it reduced by 50% and 85% respectively at 99% RH, which was attributed to the change in the pore structure by the admixture and the decrease in the surface tension of the pore water, agreeing well with the suggestions by others (**Collins and Sanjayan 2000**). In terms of compressive strength, SRA was found not to cause substantial change under 50% and 99% RH.

The use of magnesia, MgO, as a shrinkage reducing mineral additive, dates back to the mid-1970s in the construction of the Baishan concrete arch gravity dam (**Lou et al. 1998**), where it proved to be a more efficient and economical measure of controlling the shrinkage of PC than conventional admixtures (**Gao et al. 2007**). The volume compensation during the drying process was due to the chemical reaction between MgO and water forming brucite ( $\text{Mg}(\text{OH})_2$ ), which results in 118% volume increase (**Holt 2001**). The effect of MgO in the AAS systems has recently been investigated, either in terms of its varying natural content in different slag compositions (**Ben Haha et al. 2011**), or as an additive (**Shen et al. 2011**). As slags are usually produced at temperatures of 1400–1600 °C (**Shi et al. 2006**), the MgO naturally present in slags is

categorized as dead burned MgO (Pericles) (**Shand 2006**); whereas reactive grade MgO (calcined at temperature lower than 1000 °C) or hard burned MgO (calcined at 1000–1400 °C) are often chosen for use as additives.

Ben Haha et al. (**2011**) investigated the effect of natural MgO content in different slags on the performance of AAS and revealed that although the main hydration product is still C–S–H gel, MgO reacts with the slag to form hydrotalcite ( $\text{Mg}_6\text{Al}_2(\text{OH})_{16}\text{CO}_3 \cdot 4\text{H}_2\text{O}$ )-like phases, the content of which increases as the MgO content in the slag increases. They also concluded that since these hydrotalcite like phases are more voluminous than C–S–H, that they result in higher strength, hence the higher the MgO content, the higher the strength. Shrinkage performance was not studied. In the work by Fei Jin et al. (**2014**) studied the effect of addition of commercial reactive MgO on drying shrinkage and strength of AAS. They are found that MgO with high reactivity accelerated the early hydration of AAS, while MgO with medium reactivity had little effect. The drying shrinkage was significantly reduced by highly reactive MgO but it also generated severe cracking under the dry condition. On the other hand, medium-reactive MgO only showed observable shrinkage-reducing effect after one month, but the cement soundness was improved. The hydration products, analyzed by X-ray diffraction, thermogravimetric analysis and scanning electron microscopy techniques, showed that Mg was mainly incorporated in the hydrotalcite-like phases. It is concluded that the curing conditions and the time of hydrotalcite-like phases formation and their quantity are crucial to the developed strength and shrinkage reduction of MAAS, which are highly dependent on the reactivity and content of reactive MgO.

In this work, the effect of replacement of magnesium oxide with different proportions and different activities on strength and drying shrinkage of AAS was studied. The effect of addition of reactive magnesium oxide on drying shrinkage and strength of AAS was previously studied (**Shen et al. 2011**; **Fei Jin et al. 2014**). However, the effect of replacement of slag by reactive MgO on drying shrinkage and strength of activated slag pastes has not been determined to date, and constitutes the object of the present study.

## **2. MATERIALS AND METHODS OF INVESTIGATIONS**

### **2.1. Materials**

Granulated blast-furnace slag (GBFS) was purchased from Helwan Steel Company. Hydromagnesite was purchased from Arabic Chemical Company. Sodium hydroxide (SH) powder of 99% purity was obtained from Fisher Scientific Company. Liquid sodium silicate (LSS) with 17 %  $\text{Na}_2\text{O}$ , 32 %  $\text{SiO}_2$  and density of 1.46 was obtained from Arabic Science Company, Egypt.

Table 1 summarizes the chemical composition of granulated blast furnace slag, and hydromagnesite as determined by X-ray Fluorescence (XRF). The mix proportion of MgO-GBFS, alkali activator content and the calcination temperatures of hydromagnesite was presented in Table (2). Fig (1).shows the mineralogical composition of GBFS and hydromagnesite. The figure shows tat the granulated slag is mainly amorphous material and hydromagnesite is well crystalline composed of 100% hydromagnesite without any impurities. Fig. (2) shows the particle size distribution of GBFS, hydromagnesite and MgO calcined at 550, 1000 and 1250 °C. It's can be found from particle size distribution that GBFS has about 90 % < 50 $\mu\text{m}$  and 10% < 7 $\mu\text{m}$ . On

the other side, the particle size of HM is mainly lower than 15 $\mu$ m. The grain size of MgO calcined at 550 °C (< 7 $\mu$ m) is lower than those calcined at 1000 °C (< 8 $\mu$ m) and 1250 °C (< 11 $\mu$ m).

**Table 1.** Chemical compositions of hydromagnesite and granulated blast-furnace slag (GBFS), wt.%.

Oxide, %	SiO <sub>2</sub>	Al <sub>2</sub> O <sub>3</sub>	Fe <sub>2</sub> O <sub>3</sub>	CaO	MgO	Na <sub>2</sub> O	K <sub>2</sub> O	SO <sub>3</sub>	TiO <sub>2</sub>	P <sub>2</sub> O <sub>5</sub>	L.O.I	Total
<b>Hydromagnesite</b>	0.09	0.08	0.01	0.4	42.95	-	0.18	0.04	-	0.03	56.19	99.94
<b>GBFS</b>	37.81	13.14	0.23	38.70	7.11	1.03	0.19	1.19	0.40	0.17	-	99.97

**Table 2.** Mix composition of blended slag cement pastes.

Fig. (3) presents the DTA thermogram of hydromagnesite. The endotherms located

Mix symbol	MgO wt. %	GBFS, wt. %	SH, wt.%	LSS wt.%	W/C ratio	Calcination temperature, °C
<b>M0</b>	0	100	3	3	0.30	-
<b>M5-550</b>	5	95	3	3	0.30	550
<b>M10-550</b>	10	90	3	3	0.30	550
<b>M15-550</b>	15	85	3	3	0.30	550
<b>M5-1000</b>	5	95	3	3	0.30	1000
<b>M5-1250</b>	5	95	3	3	0.30	1250

at 68-280 °C are due to dehydration and dehydroxylation. The carbonate is decomposed at 425-486 °C (**Frost et al. 2008**).

According to the DTA thermogram, the hydromagnesite was calcined at 550, 1000 and 1250 °C in order to study the effect of different calcination temperatures on the reactivity and crystallinity of magnesium oxide. The MgO calcined at temperatures 550, 1000 and 1250 namely (MgO<sub>550</sub>, MgO<sub>1000</sub> and MgO<sub>1250</sub>). The calcined MgO was determined by XRD pattern (Fig. 4). The XRD diffractograms show that the increase in calcination temperature from 550 up to 1250 °C leads to enhance the crystallinity of MgO.

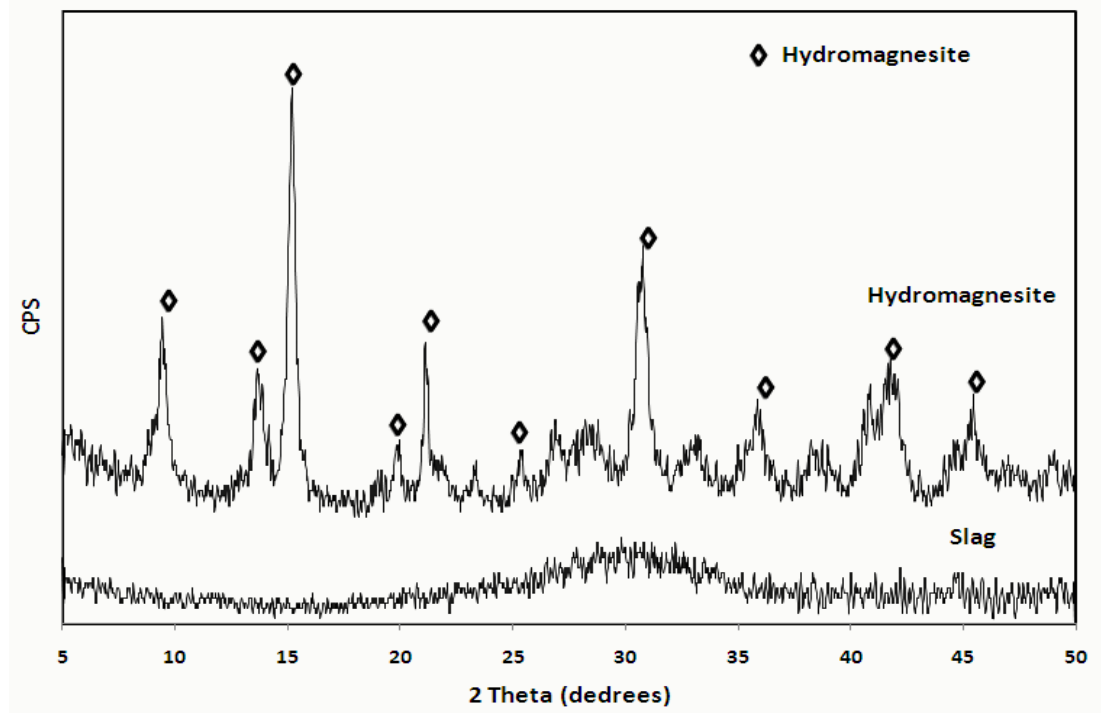


Fig. 1. XRD pattern of hydromagnesite and slag samples

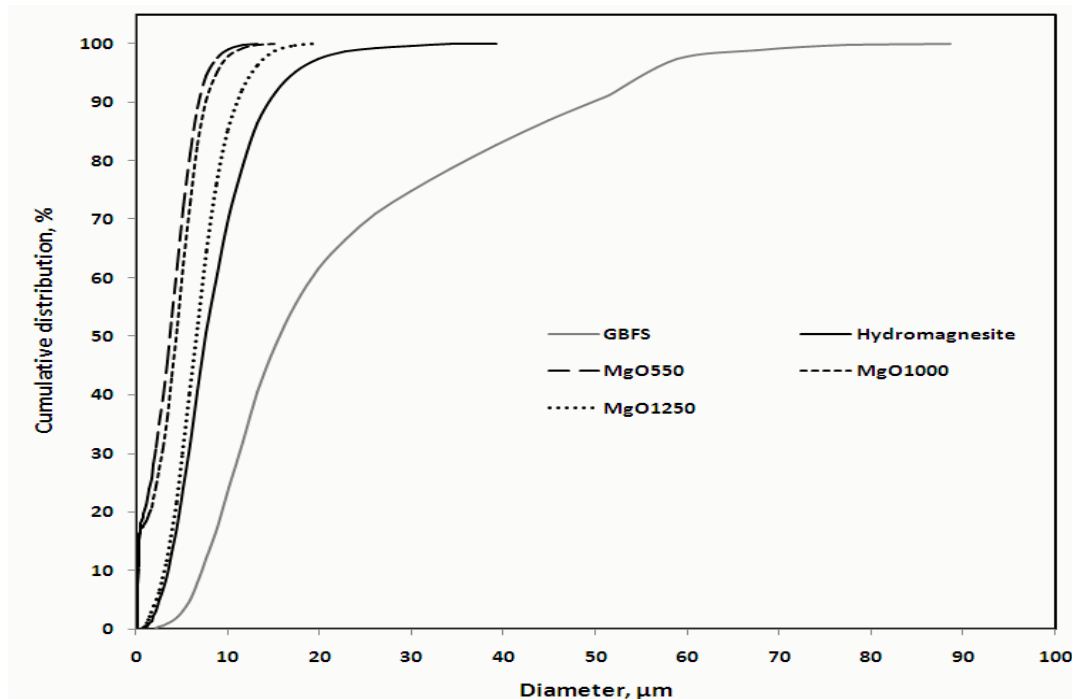
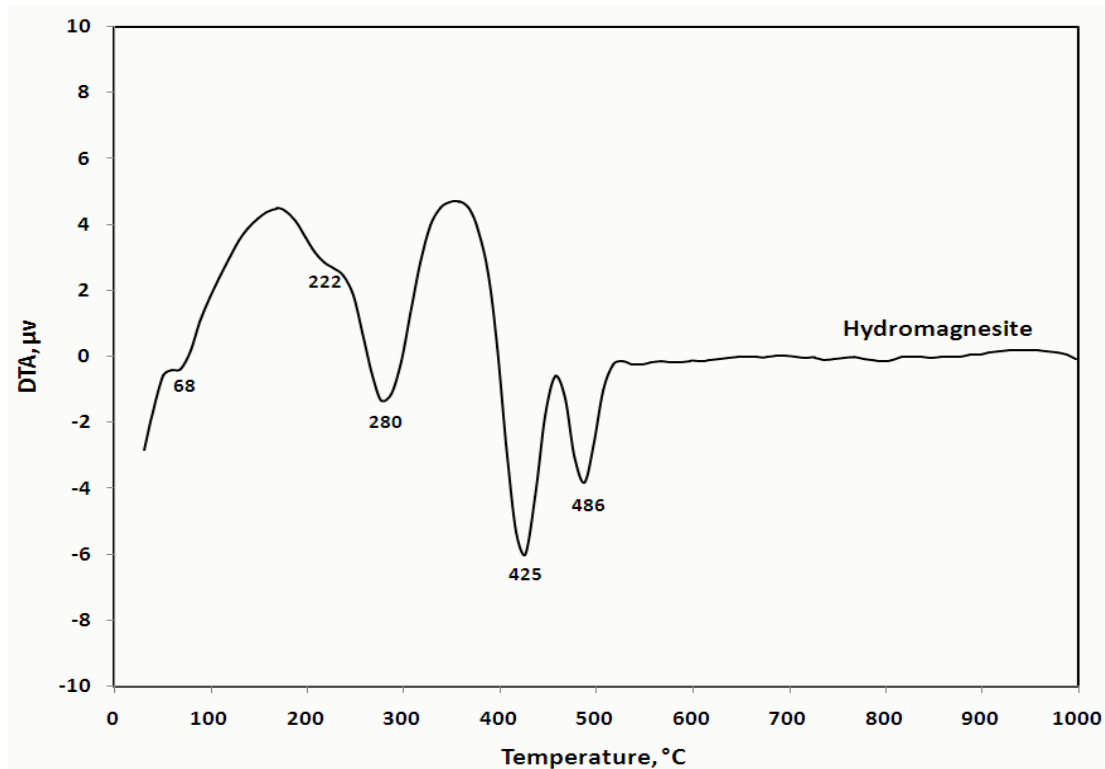


Fig. 2. Particle sizes distribution of hydromagnesite and  $MgO_{550}$ ,  $MgO_{1000}$  and  $MgO_{1250}$ .

The reactivity test was used to measure the time duration required for the neutralization of an acidic solution (0.25M acetic acid solution) by a certain MgOs (MgO550, MgO1000 or MgO1250) with mass (5.0g) and Phenolphthalein was adopted as the pH indicator (**Shand 2006**). The time from adding the MgO to the change of the solution color is recorded as the reactivity and the shorter the time, the more reactive the MgO is. The test was performed in duplicate for each sample and the average value was reported.



**Fig. 3:** DTA thermogram of hydromagnesite.

#### 2.1. 1. Alkali activated slag – MgOs psates preparation

Three MgO-AAS pastes were used in which the reactive MgO, calcined at 550 °C, content varied from 5 to 15% by mass of slag and also, two MgO-AAS paste mixes in which the 5% MgOs with different activity, MgO<sub>1000</sub> and MgO<sub>1250</sub>, were prepared. All other components were kept constant including water to solid (including the slag, reactive MgO and activators) ratio of 0.30 to ensure good workability. The MgO was first mixed with the slag for 2 min in a bench-top mixer to achieve homogeneity to which the (3:3 wt. %) NaOH: LSS solution (6% wt. of slag) was then added. The percent of NaOH and LSS was chosen as a result of previous studies (**El Didamony et al. 2010; El Didamony et al. 2012; El Didamony et al. 2013**). After mixing for another 2 min, the mix was cast into the cubic (25 × 25 × 25 mm) or prism (25×25×285 mm) moulds in two layers and hand-vibrated to eliminate air voids. The samples were then covered with cling film to avoid moisture loss. After 24 h, the samples were demoulded carefully and the cubes and prisms were transferred into the relative humidity of 99 ± 1% at 23±2 °C.

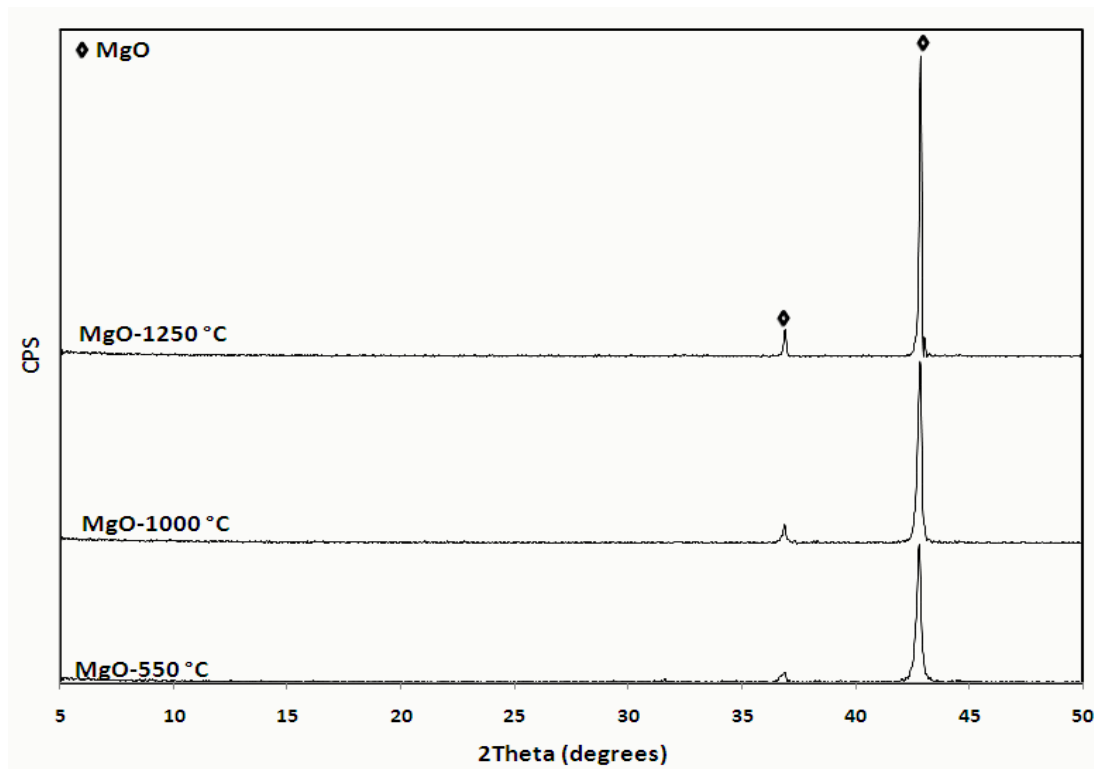


Fig.4.  
XRD

pattern of MgO calcined at 550, 1000 and 1250 °C.

## 2.2. Methods of Investigations

The compressive strength of the specimens were measured after 3, 7, 14, 28, 56 days according to ASTM C109M (2012). Shrinkage was determined as specified in American standard ASTM C490 (2007). The length change of activated slag mortar with or without magnesium oxide at any age was calculated as follows:

$$L = (L_x - L_i) / G$$

Where:

L = change in length at x age, %,  $L_x$  = comparator reading of specimen at x age minus comparator reading of reference bar at x age.  $L_i$  = initial comparator reading of specimen minus comparator reading of reference bar at that same time. G = nominal gauge length, 285 mm.

Differential thermal analysis (DTA) and thermogravimetric analysis (TGA) were carried out by heating the sample in nitrogen atmosphere up to 1000 °C with a heating rate 20 °C/min using a DT-50 Thermal Analyzer (Schimadzu Co-Kyoto, Japan). The results were compared with DTA standard data. X-ray diffraction analysis was carried out on a Philips PW3050/60 X-ray diffractometer using a scanning range from 5 to 50 with a scanning speed of 1 s/step and resolution of 0.05°/step. Infrared spectra were also recorded from 4000  $\text{cm}^{-1}$  to 400  $\text{cm}^{-1}$  using Perkin Elmer FTIR Spectrum RX1 Spectrometer. The scanning electron microphotographs were obtained with Inspect S (FEI Company, Holland) equipped with an energy dispersive X-ray analyzer (EDXA).

## 3. RESULTS AND DISCUSSION

### 3.1 Determination Reactivity Degree of MgOs.

The reactivity values (as the time increases, the reactivity decreases) of all the MgOs ( $\text{MgO}_{550}$ ,  $\text{MgO}_{1000}$  or  $\text{MgO}_{1250}$ ) powders tested is plotted in Fig. 5. It is found that the time required to neutralization of acetic acid by  $\text{MgO}_{550}$ ,  $\text{MgO}_{1000}$  and  $\text{MgO}_{1250}$  are 37 sec., 70 sec. and 163 sec. This is indicated that the  $\text{MgO}_{550}$  was more reactive than that of  $\text{MgO}_{1000}$  and  $\text{MgO}_{1250}$ . This confirms that the reactivity of the calcined MgOs is strongly affected by the thermal conditions of the calcination process (Mo et al. 2010).

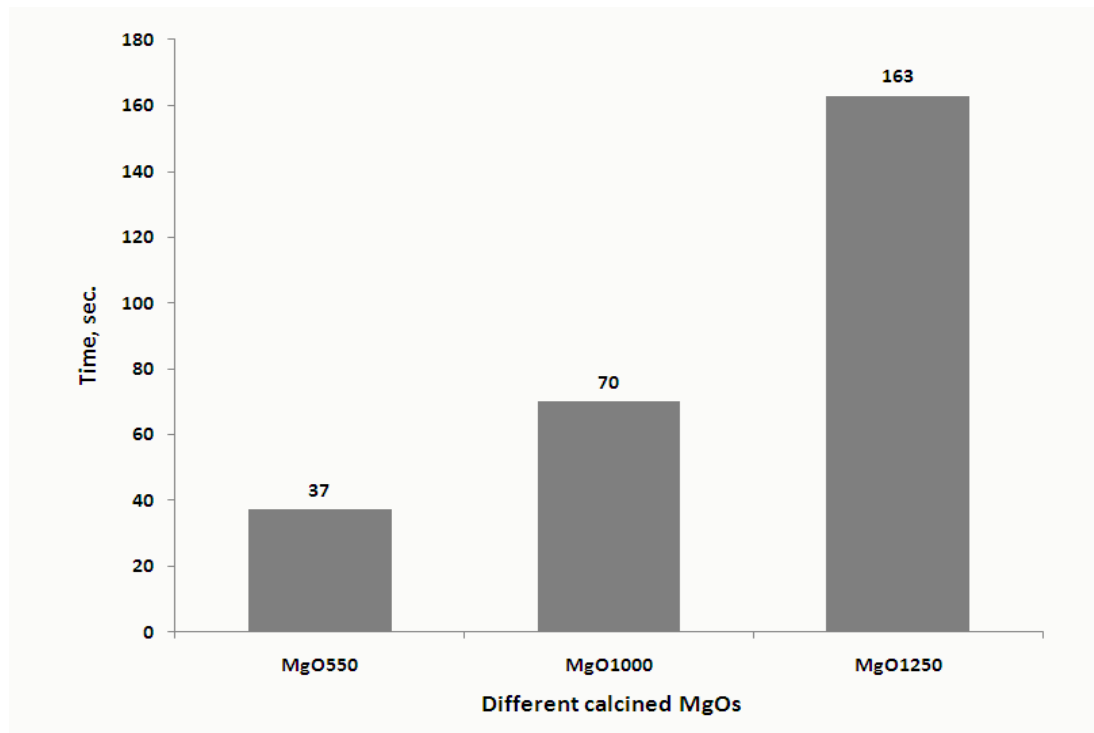
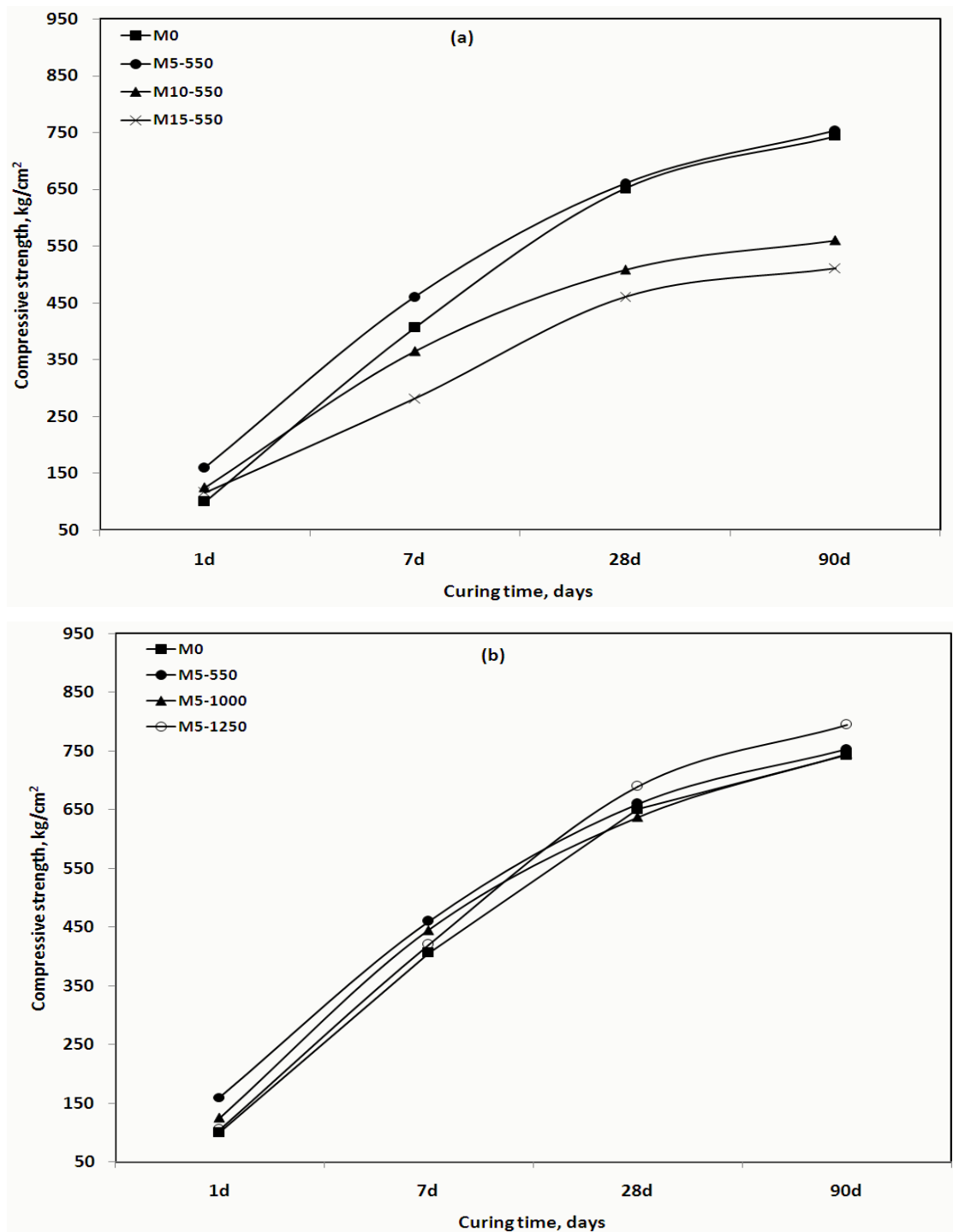


Fig.5.

Determination reactivity of MgOs by acetic acid test.

### 3.2. Compressive Strength

Fig. (6a) shows the effect of  $\text{MgO}_{550}$  contents (5, 10 and 15 %) on the compressive strength of AAS pastes. It is clear from compressive strength results that, there is significant development in the compressive strength at early ages for AAS pastes replaced by 5, 10 and 15 %  $\text{MgO}_{550}$ , respectively. Obviously, a highest increase in strength value (~26 %) was achieved for AAS paste replaced by 5 %  $\text{MgO}_{550}$  (M5-550) at 1 day. The reduction in compressive strength was observed when slag replaced by 10 and 15%  $\text{MgO}_{550}$  (M10-550 and M15-550) but still greater than that of reference sample (M0). The 5%  $\text{MgO}_{550}$  increase early ages strength up to 7days while the 10 and 15%  $\text{MgO}_{550}$  increase early ages strength for only 1day. The (M5-550) was close and showed nearly the same strength compared to the reference sample after 28 and



**Fig. 6.** Compressive strength of AAS bled with (a) 5, 10 and 15% of MgO<sub>550</sub> and (b) 5% of MgO<sub>550</sub>, MgO<sub>1000</sub> and MgO<sub>1250</sub>.

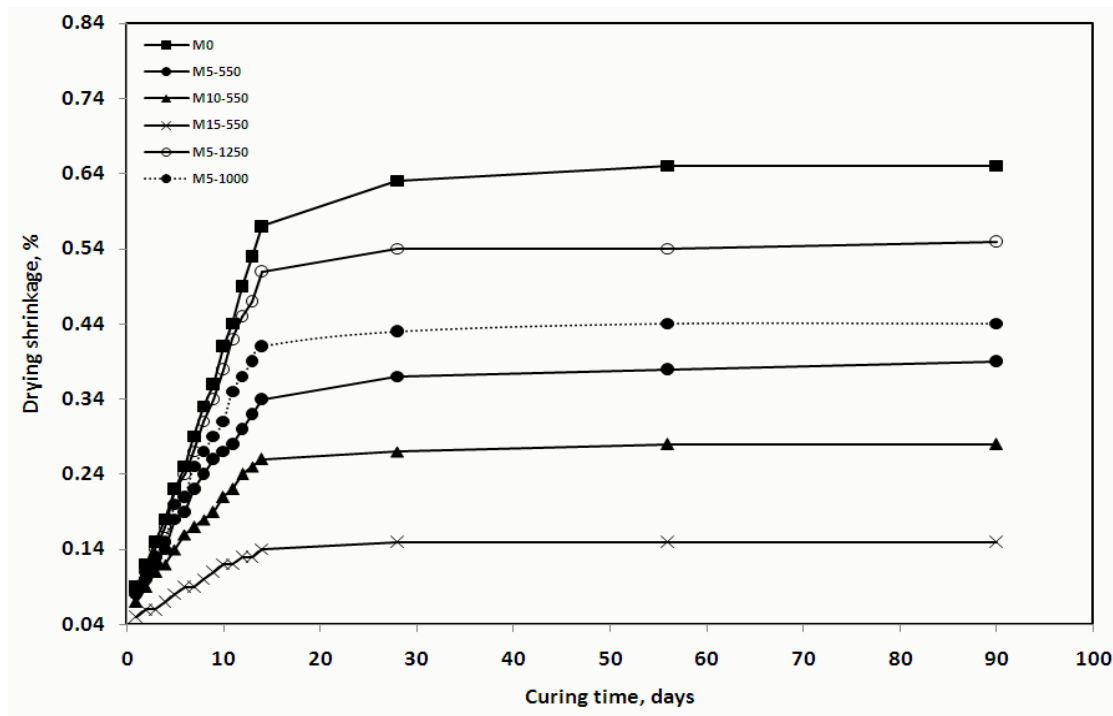
90 days. On the other side, the compressive strength values for M10-550, M15-550 was reduced by about 22%, 30% at 28 days and 25, 32% at 90 days compared to reference sample.

Fig. (6b). shows the effect of MgOs ( $\text{MgO}_{550}$ ,  $\text{MgO}_{1000}$  or  $\text{MgO}_{1250}$ ) on strength of AAS pastes. The compressive strength was slightly increased as a result of replacement of slag by 5%  $\text{MgO}_{1250}$  at early ages (1 and 7 days). The early age's compressive strength of AAS- $\text{MgO}_{550}$  blend was higher than that of the reference sample (M0) and AAS- $\text{MgO}_{1000}$  (M5-1000) and AAS- $\text{MgO}_{1250}$  (M5-1250) blends. A significant increase in strength was observed after 7 days when slag replaced by 5 %  $\text{MgO}_{1250}$ .

Finally, the highly reactive MgO accelerate the early age hydration of slag as a result of fast heat release during the dissolution process of MgO which accelerate hydration reaction leading to the formation of more hydration products (**Fei Jin et al. 2014**). **Liska (2009)** found that the heat of hydration from highly reactive MgO paste was >25 times higher than that of a less reactive MgO. It was measured that the highly reactive MgO past's temperature increased to  $\sim 100$  °C in 30 min. The replacement of slag by high content of highly reactive MgO (10 and 15 %) decreased the compressive strength at later ages. This is due to the fact that MgO reacts with broken Si-O or Al-O of AAS to form magnesium silicate hydrate or hydrotalcite like phases (Ht) leading to decrease activated species of  $\text{AlO}^{4-}$  and  $\text{SiO}^{4-}$  which act as monomers for geopolymer. In addition, the replacement of slag by high content of MgO reduces the aluminosilicate content.

### 3.3. Drying Shrinkage

Fig. (7) shows the drying shrinkage of AAS and AAS-MgO pastes up to 90 days. The drying shrinkage of AAS reduced with replacement of slag by 5, 10 and 15  $\text{MgO}_{550}$  (M5-550, M10-550 and M15-550) by  $\sim 40$ , 57 and 77%, respectively, compared to the reference specimens (M0) after 90 days. There is no great difference in the drying shrinkage of M5-1000 and M5-550 especially at later ages. In contrast, the drying shrinkage of low reactive  $\text{MgO}_{1250}$  (M5-1250) paste was nearly close to reference specimen during the first week then showing a final shrinkage (at 90 days) decreased by 15% than reference specimens. It can be concluded that, the reduction of drying shrinkage of AAS by replacement with MgO is referred to expansion by hydration and carbonation of MgO (**Shen et al. 2011**). The Ht formed as a result of hydration and carbonation of MgO which caused healing for cracks resulted from shrinkage of AAS; the healing property is attributed to lower density of Ht ( $2 \text{ g/cm}^3$ ) compared to tobermorite like CSH ( $2.23 \text{ g/cm}^3$ ), resulting in more effective pore filling and low porosity (**Ben Haha et al. 2011**). The formation rate of Ht increases with the reactivity of MgO since the quicker dissolution of MgO results in the  $\text{Mg}^{2+}$  being available in the pore water to react with broken Al-O bond within the slag by alkali activation (**Jin et al. 2013**).



**Fig. 7.** Drying shrinkage of reference specimens and AAS blended with 5, 10 and 15%  $MgO_{550}$  as well as blended with 5% of  $MgO_{1000}$  and  $MgO_{1250}$ .

### 3.4. Hydration Products and Microstructure

#### 3.4.1. XRD analysis

The major hydration products of AAS detected by XRD are Ht and CSH (Fig. 8a,b). The broad and diffuse peak at  $25-35^\circ 2\theta$  reflects the short range order of the  $CaO-Al_2O_3-MgO-SiO_2$  glass structure of the slag. Comparing Ht peak intensity at  $2\theta 11.7^\circ$  of M5-550 and M5-1250, it can be found that the intensity of Ht peak of M5-550 is higher than that of M5-1250. This is indicated that the  $MgO_{550}$  is highly reactive than  $MgO_{1250}$ . In addition, the higher content of unhydrated MgO (indicated by the higher peak at  $2\theta \sim 42.9^\circ$ ) was detected in pastes with  $MgO_{1250}$  considering its lower reactivity. Increasing the curing time did not generate new phases, but it increased the crystallinity of C-S-H as indicated by the sharper peak at around  $2\theta \sim 29.5^\circ$  (Fig. 8b) (Bernal et al. 2013). On the other side, as the contents of  $MgO_{550}$  increases the Ht peak intensity enhances. Also, the unhydrated MgO peak intensity decreases with the curing time due to formation of more Ht like phase. It should be noted that there was no brucite present in all the pastes regardless of the MgO and its content even at 1 day. According to (Yip et al. 2005; Provis et al. 2005), the activation of slag initially consists of a breakdown of the covalent bonds Si-O-Si and Al-O-Si (Zhang et al. 2011). With the reactive MgO modification, MgO hydrolysed on the surface and either reacts with the broken Si-O or Al-O to form magnesium silicate hydrate (M-S-H) or Ht, hindering

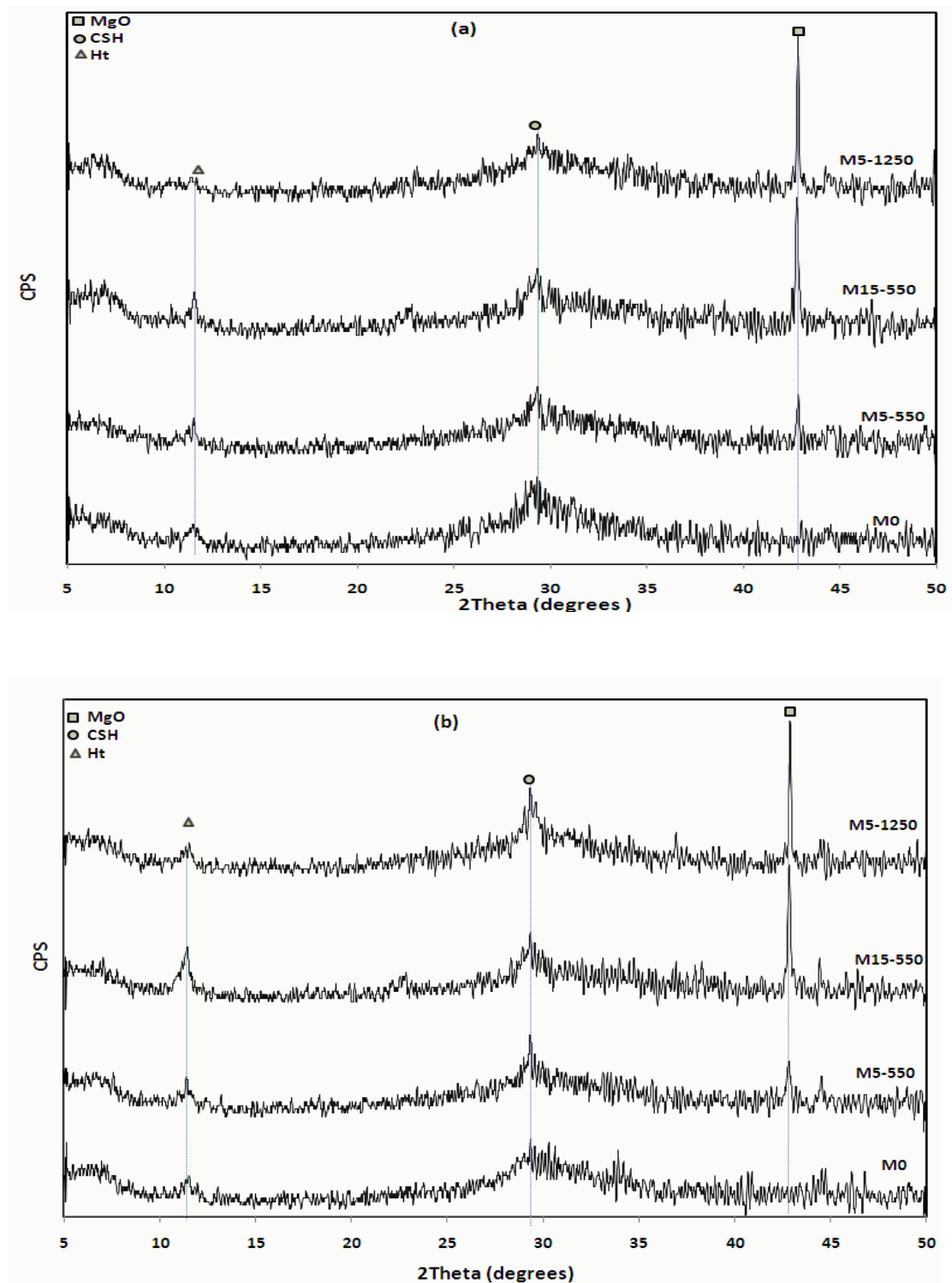


**Fig.8.** XRD diffractograms of reference specimens and AAS-MgO blends after (a) 1 day and (b) 28 days.

the precipitation of brucite. The findings here confirmed early studies that Mg is quickly consumed to form Ht or M-S-H in combination with silica fume or slag (Zhang et al., 2011; Jin and Al-Tabbaa 2013), although M-S-H is hard to be detected by XRD (Brew and Glasser 2005).

#### 3.4.2. TG/DTG analysis

The TG/DTG thermograms of pastes cured for 1 and 28 days are seen in Fig. (9a,b) and Fig. (10 a,b). From the DTG thermograms, several peaks can be observed. For temperatures up to 250 °C, the weight loss was attributed to the dehydration of C-S-H and M-S-H (Jin and Al-Tabbaa 2013; Alarconruiz et al. 2005). The temperature range of 250– 500 °C denotes the decomposition of Ht. The small peak at around 520– 570 °C was attributed to the loss of coordinated water in M-S-H (Tartaglione et al. 2008). The temperature range of 600–900 °C is the decomposition range of various carbonate-containing phases including Ht (Parashar et al. 2012), magnesium carbonate (Demir et al. 2003), and calcium carbonate (Dweck et al. 2002), originating from the raw material and the carbonation due to exposure to the air. Generally, all the weight losses increased with the increase of MgO content and the curing time, which is attributed to the higher hydration degree thus more hydration products formed. The weight loss of M15-550 (10.34 and 12.03 %) is greater than that of M5-550 (8.31 and 9.46 %) and reference specimens (7.71 and 8.89 %) for 1 day and 28 days. This is due to the fact that as MgO content increases the Ht and MSH increase as indicated in DTG curves. On the other side, the weight loss of M5-1250 specimens (7.03 %) is lower than that of M5-550 (8.31 %) at 1 day; this indicated that the low reactivity of MgO<sub>1250</sub> which leads to the formation of low amount of Ht and MSH. The weight loss of M5-1250 (10.36%) is greater than that of M0 (8.89%) and M5-550 (9.46 %) at 28 day. In conclusion, the highly reactive MgO<sub>550</sub> accelerated the hydration of slag remarkably at 1 day while the MgO<sub>1250</sub> had little effect. At 28 day, both MgO increase the rate of hydration of slag.

#### 3.4.3. FTIR analysis

Fig. (11 a,b) shows the FTIR spectra of MgO-AAS specimens at 1 day and 28 days. The results indicate that there were different absorption bands. The absorption band at 464-492 cm<sup>-1</sup> is due to O-Si-O bonds bending vibration. Additionally, relatively well-resolved band at 658-716 cm<sup>-1</sup> has appeared which is associated to the symmetric stretching vibrations of Si-O-Al bridges. The absorption bands located at 952-974 cm<sup>-1</sup> are due to Si (Al)-O asymmetric stretching vibrations. The absorption band located at 1640-1649 cm<sup>-1</sup> is due to bending H-O-H vibration and the absorption band at 3444-3469 cm<sup>-1</sup> is due to stretching of O-H groups. The absorption bands located at 1382-1465 cm<sup>-1</sup> are due to carbonate group of calcium carbonate, magnesium carbonate or Ht. It can be noted that the intensity of absorption bands characteristic for bending H-O-H vibration and stretching of O-H groups increases with increasing of curing time for all mixes. This is attributed to increase of hydration products with curing time. Obviously, the intensity of absorption bands related to symmetric stretching vibrations of Si-O-Al bridges and asymmetric stretching vibrations of Si (Al)-O decrease with increasing the

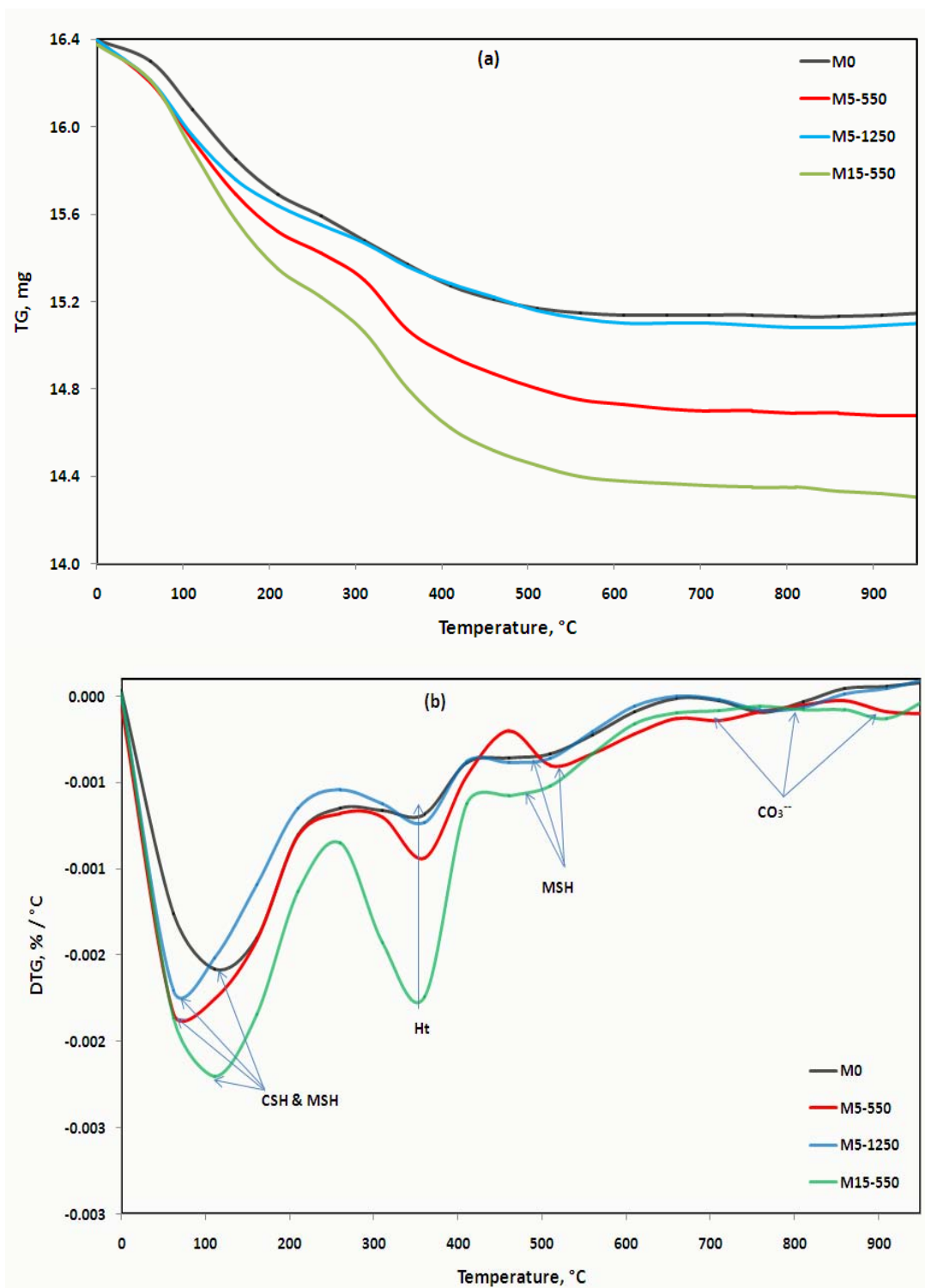


**Fig. 9.** TGA (a) and DTG (b) of AAS and AAS-MgO blends after 1 days

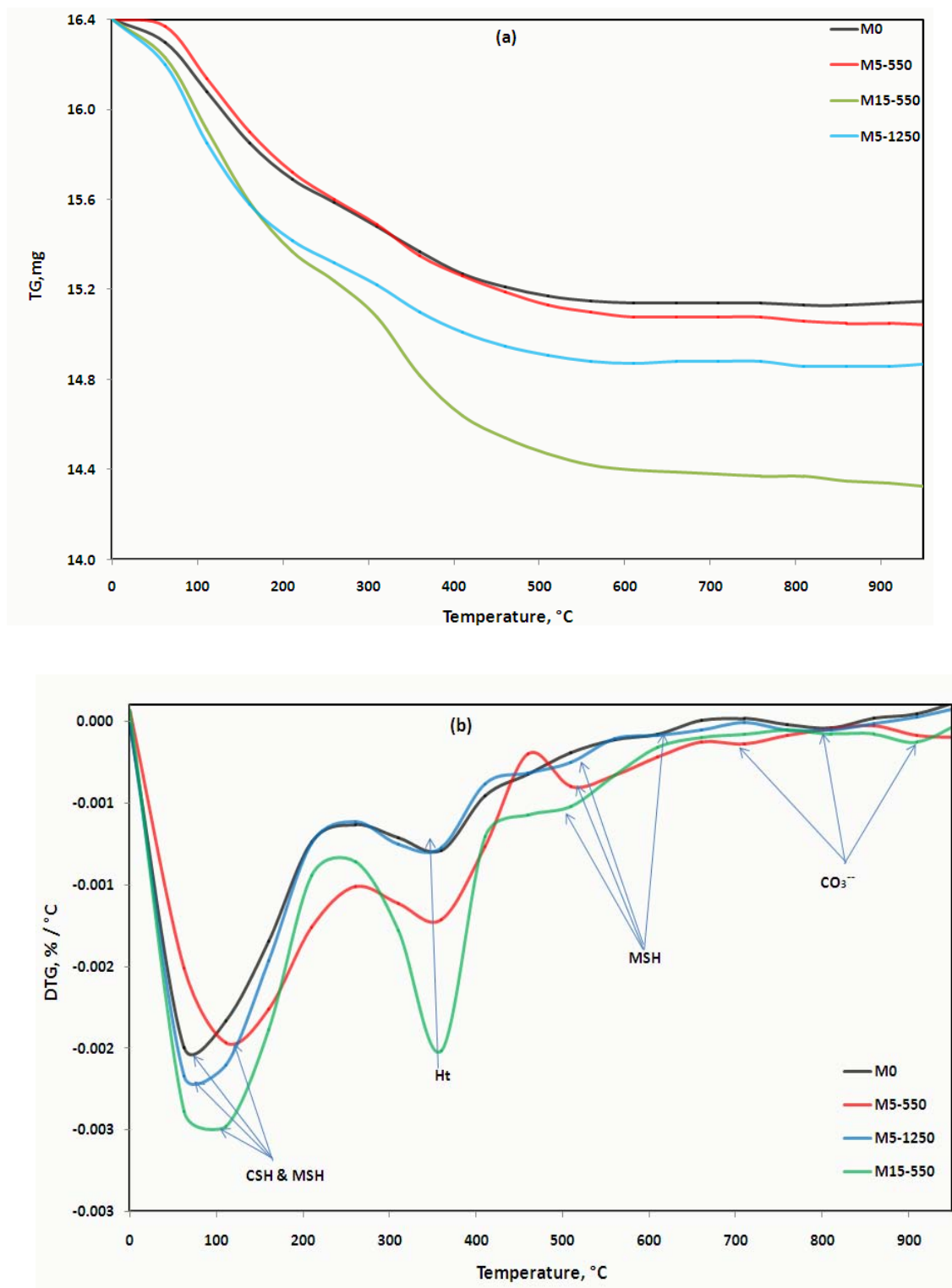


**Fig. 10.** TGA (a) and DTG (b) of AAS and AAS-MgO blends after 28 days.

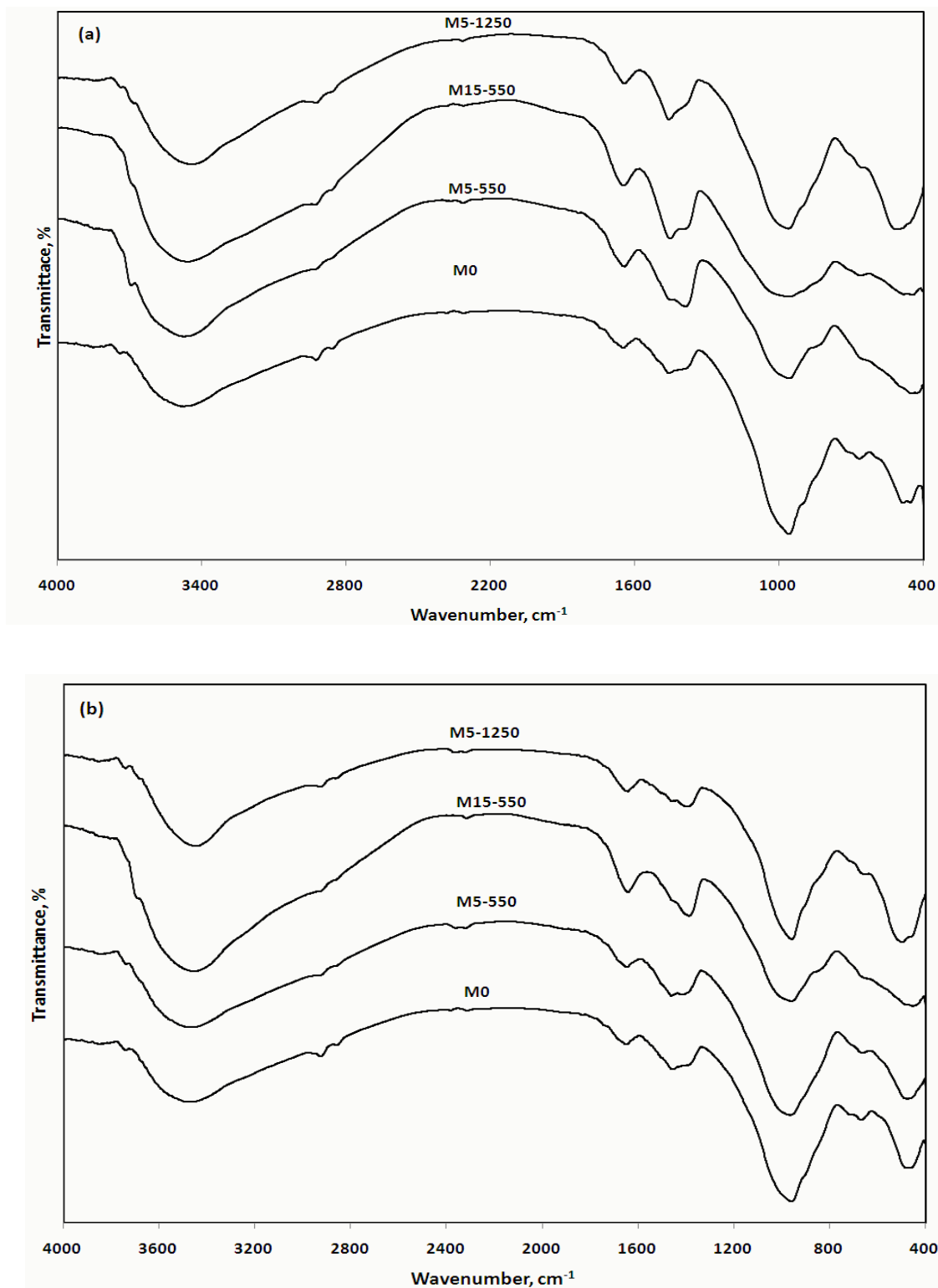


**Fig. 11.** FTIR spectra of AAS and ASS-MgO blends after (a) 1 day and (b) 28 days.

amount of  $\text{MgO}_{550}$  for 1 and 28 days of curing. This proves the reaction between activated species (Al-O and Si-O) and MgO which leads to the formation of MSH and Ht. This can be observed from the intensity of the bands related to bending H-O-H vibration and stretching of O-H groups which increases with increasing of  $\text{MgO}_{550}$  content. In addition, the replacement of slag on the expense of aluminosilicate content leads to decrease the intensity of aluminosilicate bands. In contrast, the intensity of bands related to symmetric stretching vibrations of Si-O-Al bridges and asymmetric stretching vibrations of Si (Al)-O of AAS -  $\text{MgO}_{1250}$  blend (M5-1250) are higher than those of AAS-  $\text{MgO}_{550}$  blend (M5-550) especially after 28 days. Also, the high full width at half maximum (FWHM), the low FWHM the more crystalline and ordered structure, which especially noticeable in the case of the most intense band at  $958\text{ cm}^{-1}$  of M5-1250 is lower than that of M5-550 and reference specimens (M0). This is attributed to the high crystalline (low reactive)  $\text{MgO}_{1250}$  acts as nucleation centers which accelerate the rate of crystal geopolymer formation. This indicated that the increase of strength of M5-1250 after 28 days (**Duxson et al. 2009**).

Figs. (12) shows the SEM micrograph of  $\text{MgO}$ -AAS pastes at 1 and 28 days. The microstructure of M5-550, M10-550 and M15-550 is highly compacted and more dens than that of the reference sample (M0) and M5-1250 at early age (1 day). This is mainly due to two reasons. Firstly, the replacement of slag by highly reactive  $\text{MgO}_{550}$  caused the acceleration the early age hydration of slag which leads to the formation of a dens CSH gel and therefore the highly chemically combined water was generated as shown in TG/DTG (Figs 9a,b). The gels have occupied the spaces that were initially filled with water and generated a more compact microstructure further lead to increased strength as presented in Fig. (6a ). Secondly, the  $\text{MgO}$  reacts with broken Al-O and Si-O forming Ht and M-S-H, The Ht was clearly observed in case of M5-550 and M15-550. The Ht is more voluminous than C-S-H and therefore occupies more spaces which leads to generate dens and compact microstructure. After 28 days, all pastes formed dense microstructure with cracks which observed in case of reference specimens (M0) and M5-1250.

#### 4. CONCLUSION

The main findings of this study can be summarized as follows:

- (1) The highly reactive  $\text{MgO}_{550}$  accelerated hydration and consequent increases the early compressive strength of AAS pastes while the low reactive  $\text{MgO}_{1250}$  had little effect.
- (2) The acceleration of hydration of AAS-  $\text{MgO}$  at early ages is ascribed to the heat released during the hydration of  $\text{MgO}$ .
- (3) The replacement of slag by 5% low reactive  $\text{MgO}_{1250}$  significantly improved the compressive strength at later age of curing. This is attributed to the high crystalline (low reactive)  $\text{MgO}_{1250}$  which acts as nucleation centers and accelerate the rate of geopolymer formation.
- (4) In this study, the replacement of slag by reactive magnesium oxide was much more effective in reducing the drying shrinkage of AAS than that of addition of magnesium oxide which was reported by Fei Jin et al. (**2014**).

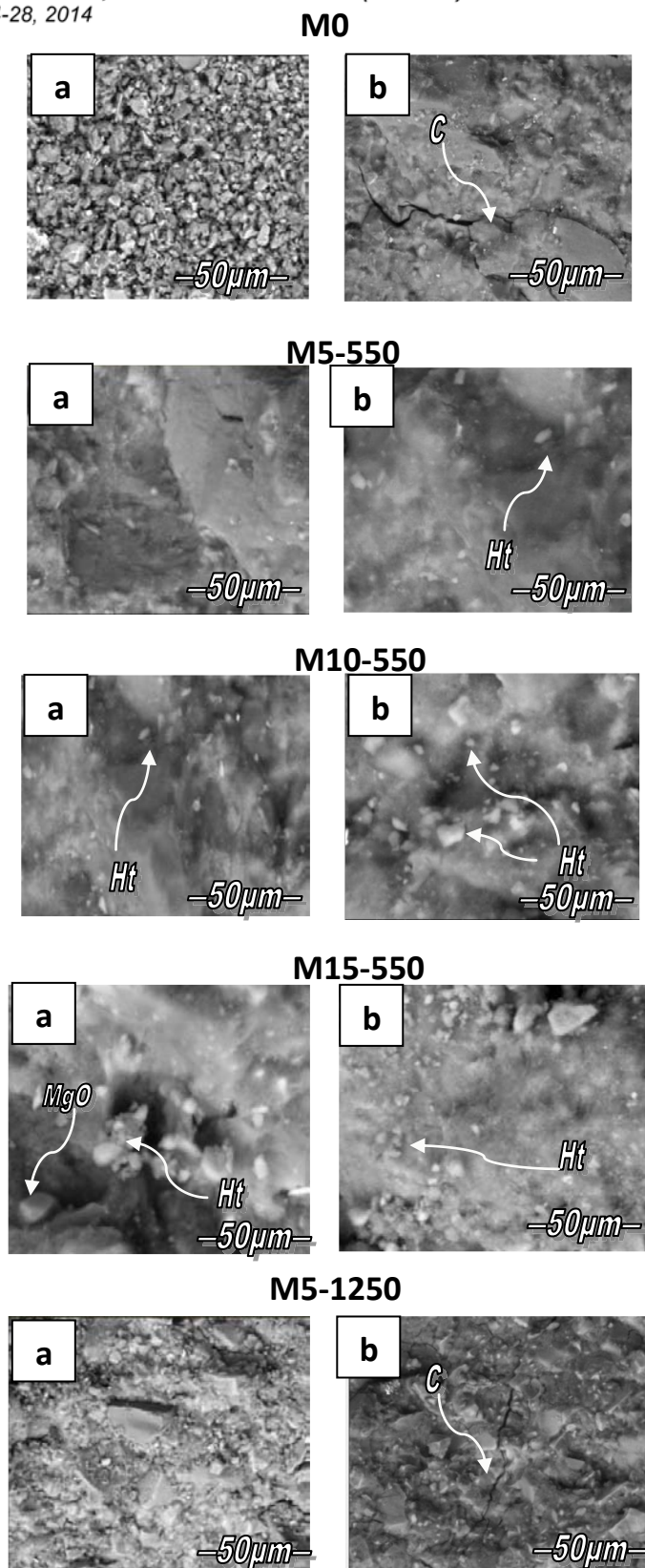


**Fig. 12.** SEM of AAS and AAS-MgO after (a) 1 day and (b) 28 days.

(5) The replacement of slag by 5, 10 and 15 %  $\text{MgO}_{550}$  reduced the drying shrinkage of AAS by ~ 40%, 57% and 77% after 90 days. Also, the drying shrinkage of M5-1000 showed nearly the same compared to M5-550 especially at later ages. In contrast, the drying shrinkage of low reactive  $\text{MgO}_{1250}$  (M5-1250) paste was close to reference specimens during the first week then showing a final shrinkage (at 90 day) decreased by 15% than the reference specimens.

(6) The MgO reacts with slag to form Ht like phases which is responsible for the reduction of drying shrinkage of AAS as indicated by XRD, TG/DTG, FTIR and SEM analyses.

## 5. REFERENCES

- Alarconruiz, L., Platret, G., Massieu, E. and Ehlacher, A. (2005), "The use of thermal analysis in assessing the effect of temperature on a cement paste." *Cem. Concr. Res.*, Vol. **35**, 609–613.
- ASTM C109M (2012), "Standard test method for compressive strength of hydraulic cement mortars."
- ASTM C490. (2007), "Standard Practice for Use of Apparatus for the determination of Length Change of Hardened Cement Paste, Mortar, and Concrete."
- Bakharev, T., Sanjayan, J.G. and Cheng, Y.B. (2000), "Effect of admixtures on properties of alkali activated slag concrete." *Cem. Concr. Res.*, Vol. **30**, 1367–1374.
- Ben Haha, M., Lothenbach, B., Le Saout, G. and Winnefeld, F. (2011), "Influence of slag chemistry on the hydration of alkali-activated blast-furnace slag—Part I: Effect of  $\text{MgO}$ ." *Cem. Concr. Res.*, Vol. **41**, 955–963.
- Bernal, S.A., Provis, J.L., Rose, V. and Gutiérrez, R.M. (2013), "High-resolution X-ray diffraction and fluorescence microscopy characterization of alkali-activated slag–metakaolin binders." *J. Am. Ceram. Soc.*, Vol. **96**, 1951–1957.
- Brew, D.R.M. and Glasser, F.P. (2005), "Synthesis and characterisation of magnesium silicate hydrate gels." *Cem. Concr. Res.*, Vol. **35**, 85–98.
- Cahit Bilim, Okan Karahan, Cengiz Duran Atis and Serhan Ilkentapar (2013), "Influence of admixtures on the properties of alkali-activated slag mortars subjected to different curing conditions." *Mat. Desig.*, Vol. **44**, 540–547.
- Cincotto MA, Melo AA, Repette WL. Effect of different activators type and dosages and relation to autogenous shrinkage of activated blast furnace slag cement, in: G. Grieve, G. Owens (Eds.), *Proceedings of the 11th International Congress on the Chemistry of Cement*, Durban 2003; 4:1878–88.
- Collins, F. and Sanjayan, J.G. (1999), "Strength and shrinkage properties of alkali activated slag concrete containing porous coarse aggregate." *Cem. Concr. Res.*, Vol. **29**, 607–610.
- Collins, F. and Sanjayan, J.G. (2000), "Effect of pore size distribution on drying shrinkage of alkali-activated slag concrete." *Cem. Concr. Res.*, Vol. **30**, 1401–1406.
- Demir, F., Donmez, B., Okur, H. and Sevim, F. (2003), "Calcination kinetic of magnesite from thermogravimetric data." *Chem. Eng. Res. Des.*, Vol. **81**, 618–622.
- Duxson, P., Provis, J.L. and van Deventer, J.S.J. (2009), "Geopolymers: Structures, processing, properties and industrial applications." Woodhead Publishing, Abingdon UK.

- Dweck, J., Ferreira da Silva, P., Büchler, P. and Cartledge, F. (2002), "Study by thermogravimetry of the evolution of ettringite phase during type II Portland cement hydration." *J Therm. Anal. Calorim.*, Vol. **69**, 179–186.
- El Didamony, H., Amer, A.A., El-Sokkary, T.M. and Abd-El-Aziz, H. (2013), "Effect of substitution of granulated slag by air-cooled slag on the properties of alkali activated slag." *Ceram. Intern.*, Vol. **39**, 171–181.
- El Didamony, H., Assal, H.H., El Sokkary, T.M. and Abdel Gawwad, H.A. (2010), "Physico-chemical properties of alkali activated slag pastes." *HBRC J.*, Vol. **6**, 47–55.
- El Didamony, H., Assal, H.H., El Sokkary, T.M. and Abdel Gawwad, H.A. (2012), "Kinetics and physico-chemical properties of alkali activated blast-furnace slag/basalt pastes." *HBRC J.*, Vol. **8**, 170–176
- El-Didamony, H., Amer, A.A. and Abd El-Aziz, H. (2012), "Properties and durability of alkali-activated slag pastes immersed in sea water." *Ceram. Inter.*, Vol. **38**, 3773–3780.
- Fei Jin, Kai Gu and Abir Al-Tabbaa. (2014), "Strength and drying shrinkage of reactive MgO modified alkali-activated slag paste." *Constr. Build. Mater.*, Vol. **51**, 395–404.
- Fernández-Jiménez, A., Puertas, F. and Palomo, J.G. (1999), "Alkali-activated slag mortars: mechanical strength behavior." *Cem. Concr. Res.*, Vol. **29** (3), 593–604.
- Frost Veronika Vágvolgyi, Ray Frost, L., Matthew Hales, Ashley Locke, János Kristóf and Erzsébet Horváth. (2008), "Controlled rate thermal analysis of hydromagnesite." *J. Therm. Anal. Calorim.*, Vol. **92**(3), 893-897.
- Gao, P., Wu, S., Lin, P., Wu, Z. and Tang, M. (2001), "Morphology of MgO hydration products under different curing conditions." *Chin J. Inorg. Chem.*, Vol. **23**, 1063–1068.
- Hikkinen, T. (1993), "The influence of slag content on the microstructure, permeability and mechanical properties of concrete Part 1 Microstructural studies and basic mechanical properties." *Cem. Concr. Res.*, Vol. **23**, 407–421.
- Holt, E.E. (2001), "Early age autogenous shrinkage of concrete." Technical Research Center of Finland, 446.
- Jin, F. and Al-Tabbaa, A. (2013), "Thermogravimetric study on the hydration of reactive MgO and silica mixture at room temperature." *Thermochim. Acta.*, Vol. **566**, 162–168.
- Jin, F., Abdollahzadeh, A. and Al-Tabbaa, A. (2013), "Effect of different MgOs on the hydration of MgO-activated granulated ground blastfurnace slag paste." In: *Proceedings of 3rd international conference on sustainable construction materials and technologies*. Kyoto, Japan.
- Kutti, T. (1992), "Hydration products of alkali-activated slag." *Proc. Int. Congr. On the Chemistry of Cement*, New Delhi. Vol. **4**, 468–474.
- Li, C., Sun, H. and Li, L. (2010), "A review: the comparison between alkali-activated slag (Si+Ca) and metakaolin (Si+Al) cements." *Cem. Concr. Res.*, Vol. **40**, 1341–1349.
- Li, Y. and Sun, Y. (2000), "Preliminary study on combined-alkali–slag paste materials." *Cem. Concr. Res.*, Vol. **30**, 963–966.
- Liska, M. (2009), "Properties and applications of reactive magnesia cements in porous blocks." PhD thesis. University of Cambridge.

- Lou, Z., Ye, Q., Chen, H., Wang, Y. and Shen, J. (1998), "Hydration of MgO in clinker and its expansion property." *J. Chin. Ceram. Soc.*, Vol. **26**, 430–436.
- Melo Neto, A.A., Cincotto, M.A. and Repette, W. (2008), "Drying and autogenous shrinkage of pastes and mortars with activated slag cement." *Cem. Concr. Res.* Vol. **38**, 565–574.
- Mo, L., Deng, M. and Tang, M. (2010), "Effects of calcination condition on expansion property of MgO-type expansive agent used in cement-based materials." *Cem. Concr. Res.*, Vol. **40**(3), 437–446.
- Palacios, M. and Puertas, F. (2007), "Effect of shrinkage-reducing admixtures on the properties of alkali-activated slag mortars and pastes." *Cem. Concr. Res.* Vol., **37**, 691–702.
- Parashar, P., Sharma, V., Agarwal, D.D. and Richhariya, N. (2012), "Rapid synthesis of hydrotalcite with high antacid activity." *Mater Lett.*, Vol. **74**, 93–95.
- Provis, J.L., Duxson, P., van Deventer, J.S.J. and Lukey, G.C. (2005), "The role of mathematical modelling and gel chemistry in advancing geopolymer technology." *Chem. Eng. Res. Des.*, Vol. **83**, 853–860.
- Rashad, A.M. (2013), "A comprehensive overview about the influence of different additives on the properties of alkali-activated slag—A guide for Civil Engineer." *Constr. Build. Mater.*, Vol. **47**, 29–55.
- Shand, M.A. (2006), "The chemistry and technology of magnesia." Hoboken, New Jersey: John Wiley & Sons.
- Shen, W., Wang, Y., Zhang, T., Zhou, M., Li, J. and Cui, X. (2011), "Magnesia modification of alkaliactivated slag fly ash cement." *J. Wuhan. Univ. Technol.-Mater. Sci.* Vol. **26**, 121–5.
- Shi, C. (1996), "Strength, pore structure and permeability of alkali-activated slag mortars." *Cem. Concr. Res.*, Vol. **26**, 1789–1799.
- Shi, C. and Day, R.L. (1996), "Some factors affecting early hydration of alkali-slag cements." *Cem. Concr. Res.*, Vol. **26**, 439–447.
- Shi, C., Krivenko, P.V. and Roy, D.M. (2006), "Alkali-activated cements and concretes." Taylor & Francis.
- Tartaglione, G., Tabuani, D. and Camino, G. (2008), "Thermal and morphological characterisation of organically modified sepiolite. Microporous Mesoporous" *Mater. J.*, Vol. **107**, 161–168.
- Wittmann, F.H. (1982), "Creep and shrinkage mechanisms. in: Bazant ZP, Witmann FH (Eds.). *Creep and shrinkage in concrete structures.*" Wiley, Chichester, 129–161.
- Yip, C.K., Lukey, G.C. and van Deventer, J.S.J. (2005), "The coexistence of geopolymeric gel and calcium silicate hydrate at the early stage of alkaline activation." *Cem. Concr. Res.*, Vol. **35**, 1688–1697.
- Young, J.F. (1988), "Physical mechanisms and their mathematical descriptions, in: Bazant ZP (Ed.). *Mathematical modelling of creep and shrinkage of concrete.*" Wiley, Chichester, 63–98.
- Zhang, T., Cheeseman, C.R. and Vandeperre, L.J. (2011), "Development of low pH cement systems forming magnesium silicate hydrate (MSH)." *Cem. Concr. Res.*, Vol. **41**, 439–442.